



**HAL**  
open science

## **FLI-1 Functionally Interacts with PIAS $\alpha$ , a Member of the PIAS E3 SUMO Ligase Family**

Emile van den Akker, Sabine Ano, Hsiu-Ming Shih, Ling-Chi Wang, Martine Pironin, Jorma J. Palvimo, Noora Kotaja, Olivier Kirsh, Anne Dejean, Jacques Ghysdael

► **To cite this version:**

Emile van den Akker, Sabine Ano, Hsiu-Ming Shih, Ling-Chi Wang, Martine Pironin, et al.. FLI-1 Functionally Interacts with PIAS $\alpha$ , a Member of the PIAS E3 SUMO Ligase Family. *Journal of Biological Chemistry*, 2005, 280 (45), pp.38035-38046. 10.1074/jbc.M502938200 . pasteur-03237002

**HAL Id: pasteur-03237002**

**<https://pasteur.hal.science/pasteur-03237002>**

Submitted on 26 May 2021

**HAL** is a multi-disciplinary open access archive for the deposit and dissemination of scientific research documents, whether they are published or not. The documents may come from teaching and research institutions in France or abroad, or from public or private research centers.

L'archive ouverte pluridisciplinaire **HAL**, est destinée au dépôt et à la diffusion de documents scientifiques de niveau recherche, publiés ou non, émanant des établissements d'enseignement et de recherche français ou étrangers, des laboratoires publics ou privés.



Distributed under a Creative Commons Attribution 4.0 International License

# FLI-1 Functionally Interacts with PIAS $\alpha$ , a Member of the PIAS E3 SUMO Ligase Family\*

Received for publication, March 17, 2005, and in revised form, August 23, 2005 Published, JBC Papers in Press, September 7, 2005, DOI 10.1074/jbc.M502938200

Emile van den Akker<sup>†1</sup>, Sabine Ano<sup>†1,2</sup>, Hsiu-Ming Shih<sup>§</sup>, Ling-Chi Wang<sup>§</sup>, Martine Pironin<sup>‡</sup>, Jorma J. Palvimo<sup>¶</sup>, Noora Kotaja<sup>||</sup>, Olivier Kirsh<sup>\*\*</sup>, Anne Dejean<sup>\*\*</sup>, and Jacques Ghysdael<sup>†3</sup>

From the <sup>†</sup>Institut Curie, CNRS UMR 146, 91405 Orsay, France, the <sup>§</sup>Institute of Biomedical Sciences, Academia Sinica, 11529 Taipei, Taiwan, the <sup>¶</sup>Department of Medical Biochemistry, University of Kuopio, FIN 70211 Kuopio, Finland, the <sup>||</sup>Institute of Biomedicine, Biomedicum Helsinki, University of Helsinki, FIN 00014 Helsinki, Finland, and the <sup>\*\*</sup>Institut Pasteur, INSERM U579, 75015 Paris, France

FLI-1 is a transcription factor of the ETS family that is involved in several developmental processes and that becomes oncogenic when overexpressed or mutated. As the functional regulators of FLI-1 are largely unknown, we performed a yeast two-hybrid screen with FLI-1 and identified the SUMO E3 ligase PIAS $\alpha$ /ARIP3 as a novel *in vitro* and *in vivo* binding partner of FLI-1. This interaction involved the ETS domain of FLI-1 and required the integrity of the SAP domain of PIAS $\alpha$ /ARIP3. SUMO-1 and Ubc9, the ubiquitin carrier protein component in the sumoylation pathway, were also identified as interactors of FLI-1. Both PIAS $\alpha$ /ARIP3 and the closely related PIAS $\beta$  isoform specifically enhanced sumoylation of FLI-1 at Lys<sup>67</sup>, located in its N-terminal activation domain. PIAS $\alpha$ /ARIP3 relocalized the normally nuclear but diffusely distributed FLI-1 protein to PIAS $\alpha$  nuclear bodies and repressed FLI-1 transcriptional activation as assessed using different ETS-binding site-dependent promoters and different cell systems. PIAS $\alpha$  repressive activity was independent of sumoylation and did not result from inhibition of FLI-1 DNA-binding activity. Analysis of the properties of a series of ARIP3 mutants showed that the repressive properties of PIAS $\alpha$ /ARIP3 require its physical interaction with FLI-1, identifying PIAS $\alpha$  as a novel corepressor of FLI-1.

FLI-1 (Friend leukemia integration-1) is an ETS (E26 transformation-specific) transcription factor that plays an essential role in the megakaryocytic, granulocytic, and erythrocytic lineages and in endothelial cell development (1–4). FLI-1 shares, with other ETS family members, a conserved ETS domain responsible for nuclear targeting and specific binding to DNA elements containing a consensus GGA(A/T) core (ETS-binding site (EBS)<sup>4</sup>) (for review, see Ref. 5). FLI-1 also possesses a pointed/SAM domain embedded in its major N-terminal activation domain and a C-terminal domain that also contributes to its

transcriptional activation properties (for review, see Ref. 5). Consistent with its biochemical and biological functions, a number of genes specific to the megakaryocytic, granulocytic, and erythrocytic lineages have been found to be down-regulated in FLI-1-deficient bone marrow cells, with a subset of these genes being direct transcriptional targets of FLI-1 (Refs. 1, 3, and 4, and references therein). Remarkably, lineage-restricted expression of many megakaryocyte-specific genes relies on the cooperation between FLI-1 and GATA-1 on composite DNA elements present in their promoter/enhancer sequences (Ref. 6 and references therein). Depending on the cell and promoter contexts, FLI-1 can also repress EBS-driven transcription through ill characterized mechanisms (7, 8). Finally, FLI-1 can interact in *trans* with other transcriptional regulators, including nuclear hormone receptors and erythroid-specific Krüppel-like factor, thereby modifying transcriptional output in pathways involving these factors (9, 10).

*Fli-1* was originally identified as a common proviral integration site in erythroleukemia induced in newborn mice by the Friend murine leukemia virus component of the Friend virus complex (for review, see Ref. 5). Consistent with its central role in Friend murine leukemia virus-induced erythroleukemia, enforced expression of FLI-1 in primary erythroblasts and erythroleukemic cell lines has been shown to strongly interfere with the normal, erythropoietin-induced differentiation of these cells (8, 11), an activity that requires its EBS-dependent transcriptional activation properties (12, 13). Other studies show that FLI-1 might also contribute to the transformed phenotype through interference with the expression of genes important to erythroblast differentiation (8, 10, 14). *FLI-1* is rearranged in Ewing sarcoma (a childhood pediatric tumor of neuroectodermal origin) as a result of a t(11;22)(q24;q12) chromosomal translocation that fuses the 5'-end of the *EWS* gene to the 3'-end of *FLI-1* and the expression of a chimeric *EWS-FLI-1* protein endowed with abnormal transcriptional regulatory properties and transforming activity (for review, see Ref. 15).

PIAS1 (protein inhibitor of activated STAT proteins) and PIAS3 have been identified as inhibitors of the cytokine receptor/JAK (Janus kinase)-induced activation of STAT1- and STAT3-DNA binding, respectively. In mammals, the PIAS family also includes PIAS $\alpha$ , PIAS $\beta$ , and PIAS $\gamma$ . PIAS proteins share three conserved domains: an N-terminal SAP (SAF/Acinus/PIAS) domain, a central RING finger-like domain, and a C-terminal serine/acidic residue-rich domain. The SAP domain binds AT-rich DNA sequences known as the scaffold or nuclear matrix attachment region, involved in the topological organization of chromatin and in the regulation of gene expression (for review, see Ref. 16). The RING finger-like domain of PIAS proteins is instrumental in their ability to function as SUMO E3 ligases that favor the covalent modification of a variety of target proteins by the three known members of the SUMO (small ubiquitin-like modifier) family (for review, see Ref.

\* This work was supported in part by CNRS, the Institut Curie, the Ligue Nationale contre le Cancer (Equipe Labellisée La Ligue 2004), and the Association for International Cancer Research (to J.G.) and by the Academy of Finland (to J.J.P.). The costs of publication of this article were defrayed in part by the payment of page charges. This article must therefore be hereby marked "advertisement" in accordance with 18 U.S.C. Section 1734 solely to indicate this fact.

<sup>1</sup> Both authors contributed equally to this work.

<sup>2</sup> Supported by a predoctoral fellowship from the Ministère de l'Éducation Nationale et de la Recherche and the Association pour la Recherche contre le Cancer.

<sup>3</sup> To whom correspondence should be addressed: Institut Curie, Centre Universitaire, CNRS UMR 146, Bat. 110, 91405 Orsay, France. Tel.: 33-1-6986-3152; Fax: 33-1-6907-4525; E-mail: Jacques.Ghysdael@curie.u-psud.fr.

<sup>4</sup> The abbreviations used are: EBS, ETS-binding site; STAT, signal transducer and activator of transcription; E3, ubiquitin-protein isopeptide ligase; E1, ubiquitin-activating enzyme; E2, ubiquitin carrier protein; ERK2, extracellular signal-regulated kinase-2; HA, hemagglutinin; Gal4AD, Gal4 activation domain; GST, glutathione S-transferase; wt, wild-type; Luc, luciferase; m, mouse; PBS, phosphate-buffered saline.

## FLI-1 Functionally Interacts with PIAS $\alpha$

17). Sumoylation is a three-step process similar to protein ubiquitylation, involving a SUMO-activating enzyme (E1; AOS1/UBA2); a SUMO carrier protein (E2; Ubc9); and E3 ligases, including Ran-binding protein-2, Polycomb-2, and PIAS proteins. Sumoylation regulates a number of protein-protein interactions involved in critical cellular functions, including protein stability, nuclear import, transcriptional regulation, biogenesis of subnuclear bodies, and chromosome structure.

As the functional regulators of FLI-1 are largely unknown, we performed a yeast two-hybrid screen to identify novel FLI-1 interactors. We identified PIAS $\alpha$ /ARIP3 as a new partner and co-regulator of FLI-1. ARIP3 was found to interact physically with FLI-1, to repress its transcriptional activity, and to sequester it into PIAS $\alpha$ /ARIP3 nuclear bodies. FLI-1 is sumoylated at a single lysine residue in its transcriptional activation domain, and ARIP3 is shown to be a SUMO E3 ligase for FLI-1 *in vivo* and *in vitro*. Interestingly, the repressive properties of ARIP3 are not dependent upon its SUMO ligase activity and FLI-1 sumoylation, but critically depend upon its ability to physically complex FLI-1 into a transcriptionally inactive protein complex.

### EXPERIMENTAL PROCEDURES

**Reagents**—Anti-FLI-1 (catalog no. sc-356) and anti-ERK2 (catalog no. sc-154) antibodies were purchased from Santa Cruz Biotechnology, Inc. Anti-FLAG antibody (catalog no. F-3164) was purchased from Sigma, and anti-hemagglutinin (HA; catalog no. 1667475) was from Roche Applied Science. The anti-pan ETS antibody was a kind gift from Dr. N. Bhat. Anti-ARIP3 antibody has been described previously (18).

**Yeast Two-hybrid Screen**—The DNA fragment encoding FLI-1-(225–373) was subcloned in-frame with the LexA DNA-binding domain in the BTM116 vector to produce the bait for yeast two-hybrid studies. A human bone marrow cDNA library fused to the Gal4 activation domain (Gal4AD) was from Clontech. Yeast two-hybrid screening was performed as described previously (19), and a total of  $5 \times 10^6$  transformants were screened. Positive clones were selected on plates lacking uracil, histidine, tryptophan, lysine, and leucine, followed by  $\beta$ -galactosidase assays, and verified by one-on-one transformation assays.

**DNA Constructs**—To obtain the glutathione S-transferase (GST)-FLI-1-(3–208), GST-FLI-1-(3–286), GST-FLI-1-(188–452), and GST-FLI-1-(250–452) fusion proteins, the corresponding regions were PCR-amplified from the human *FLI-1* cDNA using pBS-wtFLI-1 (13) as a matrix with 5'-CCG TCG ACG GGA CTA TTA AGG AGG CTC TGT CG-3' as the forward primer and 5'-GGG TCG ACG GTG TGG GAG GTT GTA TTA TAG G-3' and 5'-GGG TCG ACA GGA ATT GCC ACA GCT GGA TCT GC-3' as the reverse primers for FLI-1-(3–208) and FLI-1-(3–286), respectively, and 5'-CCG GAT CCT TGT CAC ACC TCA GTT ACC TCA GG-3' and 5'-CCG GAT CCA TCA GTA AGA ATA CAG AGC AAC G G-3' as the forward primers for FLI-1-(188–452) and FLI-1-(250–452), respectively, and 5'-GGG TCG ACA AGC TTC TAG TAG TAG CTG CC-3' as the reverse primer. This resulted in flanking the PCR-amplified fragment either with a *Sall* restriction site for FLI-1-(3–208) and FLI-1-(3–286) or with *Bam*HI and *Sall* for the fragments encoding FLI-1-(188–452) and FLI-1-(250–452) at their 5'- and 3'-ends, respectively. The respective *Sall*- or *Bam*HI/*Sall*-digested PCR fragments were inserted in *Sall*- or *Bam*HI/*Sall*-cut pGEX-4T. To generate pBS-HA-wtFLI-1,  $\Delta$ EB-HA-FLI-1 (20) was partially digested with *Sst*I and *Eco*RI and ligated into *Sst*I/*Eco*RI-restricted pBluescript. Mutants FLI-1(K67R) and FLI-1(K217R) were generated by oligonucleotide site-directed mutagenesis with the QuikChange kit (Stratagene) following the manufacturer's instructions using pBS-HA-wtFLI-1 as a matrix and mutagenic primers 5'-GGG TCA ACG TCA

GGC GGG AGT ATG ACC-3'/5'-GGT CAT ACT CCC GCC TGA CGT TGA CCC-3' and 5'-CCT CAC GAT TGA GTG TCA GAG AAG ACC CTT CTT ATG AC-3'/5'-GTC ATA AGA AGG GTC TTC TCT GAC ACT CAA TCG TGA GG-3', respectively. The double point mutant FLI-1(K67R,K217R) was generated using pBS-HA-FLI-1(K67R) as a matrix and the mutagenic primers used for FLI-1(K217R). To generate HA-tagged versions of these mutants in the corresponding  $\Delta$ EB expression vector derivatives, mutagenized FLI-1 inserts were retrieved by *Xho*I/*Hind*III digestion and ligated into *Xho*I/*Hind*III-restricted  $\Delta$ EB-HA (21). The expression vectors pSG5-His-SUMO-1 and pSG5-His-HA-SUMO-2 (22) and the pFLAG expression vectors encoding wild-type (wt) ARIP3, ARIP3-( $\Delta$ 13–28), ARIP3-( $\Delta$ 1–102), ARIP3-( $\Delta$ 102–207), ARIP3-( $\Delta$ 198–337), ARIP3-( $\Delta$ 347–418), ARIP3-( $\Delta$ 346–475), ARIP3-( $\Delta$ 467–547), ARIP3-( $\Delta$ 467–487), and ARIP3(W383A) as well as *in vitro* translatable pTag2A-wtARIP3, pTag2A-ARIP3-( $\Delta$ 102–207), pTag2A-ARIP3-( $\Delta$ 347–418), and pTag2A-MIZ/PIAS $\beta$  have been described previously (23, 24). To generate pTag2A-ARIP3-( $\Delta$ 13–28), pTag2A-ARIP3-( $\Delta$ 198–337), and pTag2A-ARIP3-( $\Delta$ 346–475), the *Sma*I/*Bgl*II cDNA inserts from the respective pFLAG vectors were subcloned into *Eco*RV/*Bam*HI-restricted pTag2A (Stratagene). The  $\Delta$ EB expression plasmids encoding HA-wtFLI-1, HA-FLI-1-(276–373), tkD2A-luciferase (Luc), and mouse (m) FLI-1(-270/-41)-Luc have been described previously (12, 13). FLI-1-(273–452) was made as follows. Using  $\Delta$ EB-HA-wtFLI-1 as a template, the FLI-1 DNA fragment corresponding to amino acids 273–452 was amplified using oligonucleotides 5'-GCC TCG AGG CCT GGA AGC GGG CAG ATC C-3' (containing a 5'-*Xho*I site) and 5'-CCA AGC TTC TAG TAG TAG CTG CC-3' (containing a 3'-*Hind*III site). The amplified DNA fragment was digested with *Xho*I and *Hind*III and ligated in-frame into *Xho*I/*Hind*III-digested  $\Delta$ EB-HA to generate  $\Delta$ EB-HA-FLI-1-(273–452). pSG513-3 $\times$ HA-BirA was a kind gift from Dr. T. B. van Dijk (Erasmus Medical Center). pcDNA3-biopeptide-FLI-1(M34A) was generated as follows. An oligonucleotide encoding the biopeptide (MASSMRQLDSQKMEWRNAGGS), 5'-CCG ATA TCC CAC CAT GGC CTC TTC CCT GAG ACA GAT CCT CGA CAG CCA GAA GAT GGA GTG GCG CTC CAA CGC AGG AGG CTC TAG ATC TCC C-3', was used as a PCR template with 5'-CCC GAT ATC CCA CCA TGG-3' (containing a 5'-*Eco*RV site) and 5'-GGG AGA TCT AGA GCC TCC-3' (containing a 3'-*Bgl*II site) as primers, and the PCR product was ligated into pCR2.1-TOPO, generating pCR2.1-TOPO-biopeptide. pCR2.1-TOPO-biopeptide was digested with *Eco*RV and *Bgl*II, and the fragment was ligated into *Eco*RV/*Bgl*II-digested pBS-HA-FLI-1, replacing, in-frame, the HA tag with the biopeptide tag. wtFLI-1 contains an alternative translation initiation codon at position 34. To prevent alternative translation from AUG at position 34, this codon was mutated into an alanine codon using a site-directed mutagenesis kit and primers 5'-GGA CTC CCC GAG GCA GTC GCG TCG GCC TTG GGG AGA TGG-3' and 5'-CCA TCA CCC CAA GGC CGA CGC GAC TGC CTC GGG GAG TCC-3'. Biopeptide-FLI-1(M34A) was released from the pBS vector by digestion with *Hind*III and ligated into *Hind*III-digested pcDNA3 to generate pcDNA3-biopeptide-tagged FLI-1(M34A), referred to as biotagged FLI-1 under "Results." HA-ARIP3 was made as follows. Using FLAG-ARIP3 as a template, *wtarip3* cDNA was amplified and fused N-terminally to an HA epitope by PCR with primers 5'-GGA GAT CTG CAA CCA TGT ACC CAT ACG ATG TTC CAG ATT ACG CGG CGG ATT TCG AGG AGT TGA GG-3' (containing a 5'-*Bgl*II site), followed by the cDNA encoding the HA epitope fused in-frame to the first 20 nucleotides of wtARIP3 and 5'-CGG AAT TCT CAC TGT TGC ACA GTA TCA GA-3' (containing a 3'-*Eco*RI site). The PCR product was cut with

BglII and EcoRI and ligated into BamHI/EcoRI-digested pcDNA3, yielding pcDNA3-HA-wtARIP3.

**Affinity Chromatography of Biotinylated Proteins and Immunoprecipitation and Western Blot Analyses**—293 cells ( $1.0 \times 10^6$ ) were seeded in 60-mm<sup>2</sup> Petri dishes 24 h prior to transfection, and DNA was transfected using the calcium phosphate coprecipitation method as described previously (25). 48 h after transfection, cells were washed twice with ice-cold phosphate-buffered saline (PBS), lysed in ice-cold lysis buffer (20 mM Tris-HCl (pH 8.0), 137 mM NaCl, 10 mM EDTA, 50 nM NaF, 1% (v/v) Nonidet P-40, 10% (v/v) glycerol, 2 mM Na<sub>3</sub>VO<sub>4</sub>, 1 mM Pefabloc (Roche Applied Science), 50 mg/ml aprotinin, 50 mg/ml leupeptin, 50 mg/ml bacitracin, and 50 mg/ml iodoacetamide) on ice for 10 min, frozen in liquid nitrogen, and stored at  $-80^\circ\text{C}$  until used. Lysates were thawed on ice and cleared by centrifugation at 15,000 rpm for 10 min at  $4^\circ\text{C}$ . For immunoprecipitations, lysates were incubated for 1 h with 1  $\mu\text{g}$  of a specific IgG as indicated in the legends, followed by a 1-h incubation with 15  $\mu\text{l}$  of 50% protein A-agarose bead slurry (Amersham Biosciences). The beads were washed three times with ice-cold lysis buffer, followed by one washing step with ice-cold PBS and boiling in SDS-PAGE sample buffer for 5 min. For affinity chromatography of biotinylated FLI-1, lysates were incubated for 1 h with 10  $\mu\text{l}$  of magnetic polystyrene beads covalently coupled to streptavidin (Dynabeads M-280; 50% slurry washed three times and reconstituted in ice-cold lysis buffer). Magnetic beads were washed three times as described above for immunoprecipitation assays, except that a magnet (catalog no. Z5342, Promega Corp.) was used for fast recovery of the beads. SDS-PAGE and Western blotting were performed as described previously (26). Membranes were stripped in 63 mM Tris-HCl (pH 6.1), 2% SDS, and 100 mM  $\beta$ -mercaptoethanol for 30 min at  $50^\circ\text{C}$ , after which they were reused. When appropriate, fluorescence was detected using GeneSnap Version 6.01 (SYNGENE, Cambridge, UH) and quantified with GeneTools software (SYNGENE). Images were processed using Adobe Photoshop Version 6.0.

**Luciferase Assays and Immunofluorescence Analyses**—For transactivation experiments,  $3 \times 10^5$  HeLa or 293 cells grown in Dulbecco's modified Eagle's medium supplemented with 10% fetal calf serum (Invitrogen) were plated in six-well plates and transfected 24 h later with the indicated amount of plasmid DNA by calcium phosphate coprecipitation of DNA as described above. The total amount of expression plasmid was kept constant by addition of the corresponding empty vector without insert, and the total amount of DNA (20  $\mu\text{g}/500 \mu\text{l}$ ) was kept constant by addition of carrier plasmid DNA. Cell lysates were prepared 24 h after transfection and assayed for luciferase activity using the luciferase assay system kit (Promega). The results shown are the mean of at least three independent transfection experiments.

For immunofluorescence analyses,  $1.5 \times 10^5$  293 cells were seeded per well in 12-well plates containing 14-mm<sup>2</sup> glass coverslips (Marienfeld MultiMedia GmbH, Essen, Germany). After 24 h, cells were transfected with 1  $\mu\text{g}$  of  $\Delta\text{EB-HA-FLI-1}$  and 1.5  $\mu\text{g}$  of pFLAG-ARIP3 and mutants derived thereof as indicated using the calcium phosphate coprecipitation method. The total amount of expression plasmid was kept constant by addition of the corresponding empty vector without insert, and the total amount of DNA (20  $\mu\text{g}/500 \mu\text{l}$ ) was kept constant by addition of carrier plasmid DNA. 2 days after transfection, the cells were washed two times with PBS, fixed with 4% paraformaldehyde in PBS (15 min), and permeabilized by incubation in 0.3% Triton X-100 (15 min). After washing with PBS, the cells were incubated for 1 h with a 1:200 dilution of anti-FLI-1 antibody and a 1:100 dilution of anti-FLAG antibody in PBS containing 10% fetal calf serum at  $37^\circ\text{C}$ . Cells were washed three times with PBS and incubated for 1 h at  $37^\circ\text{C}$  with fluo-

rescein isothiocyanate-conjugated goat anti-rabbit immunoglobulin (1:100 dilution), Texas Red-coupled donkey anti-mouse antibody (1:100 dilution), and 50  $\mu\text{g}/\text{ml}$  Hoechst dye (all obtained from Jackson ImmunoResearch Laboratories, Inc.) diluted in PBS containing 10% fetal calf serum. Coverslips were washed two times with PBS and mounted in Dabco. Pictures of fixed cells were collected using a three-dimensional deconvolution imaging system. In brief, a Leica DM RXA microscope equipped with a piezoelectric translator (PIFOC, Physik Instrumente L. P.) placed at the base of a  $\times 100$  PlanApo numerical aperture 1.4 objective and a 5-MHz Micromax 1300Y interline CCD camera (Roper Instruments) was used. Stacks of conventional fluorescent images were collected automatically at 0.2- $\mu\text{m}$  z-intervals (MetaMorph software, Universal Imaging Corp.). Wavelength selection was achieved by switching to the corresponding motorized selective Leica filter block before each stack acquisition. Automated batch deconvolution of each z-series was computed using a measured point spread function with a custom-made software package (J. B. Sibarita, Institut Curie).

**DNA Binding by Electrophoretic Mobility Shift Assays and Oligonucleotide Pull-down Assay**—Electrophoretic mobility shift assays were performed essentially as described previously (20). For the oligonucleotide pull-down assay, a double-stranded DNA oligonucleotide corresponding to a high affinity FLI-1-binding site (wild-type, 5'-TCG GGT CGA CAT AAC CGG AAG TGG GC-3' ((+)-strand), with the EBS core sequence underlined) was synthesized as a 5'-biotinylated derivative. A version of this oligonucleotide mutated in the EBS core (5'-TCG GGT CGA CAT AAC **CCC** AAG TGG GC-3' ((+)-strand), with the mutations shown in boldface) was used as a negative control. The oligonucleotides were immobilized on streptavidin beads by overnight incubation at  $4^\circ\text{C}$  in binding buffer (10 mM Tris-HCl (pH 8.0), 10% glycerol, 6 mM MgCl<sub>2</sub>, 5 mM dithiothreitol, 0.1 mM EDTA, 0.01% Nonidet P-40, and 10  $\mu\text{g}/\mu\text{l}$  poly(dI·dC)) supplemented with 1% bovine serum albumin at a final ratio of 0.6  $\mu\text{g}$  of oligonucleotide/ $1 \times 10^6$  beads. After three washes, the EBS oligonucleotide-streptavidin beads were equilibrated in binding buffer. The efficiency of oligonucleotide loading onto the streptavidin beads was checked in a small aliquot by detaching the EBS from the beads by incubation at  $90^\circ\text{C}$  in 0.1% SDS and resolving the extract on a 1.5% agarose gel in the presence of ethidium bromide. Whole cell extracts were obtained (100-mm<sup>2</sup> Petri dish in 300  $\mu\text{l}$  of lysis buffer) from 293 cells transfected with the expression vector for HA-FLI-1 (1  $\mu\text{g}$ ) with or without the expression vector for HA-ARIP3 (1  $\mu\text{g}$ ) or empty vector as a control. Lysates (100  $\mu\text{l}$ ) were diluted with 2 volumes of binding buffer, keeping poly(dI·dC) constant at 10  $\mu\text{g}/\mu\text{l}$ , and incubated with  $7 \times 10^6$  oligonucleotide-immobilized beads for 60 min at  $4^\circ\text{C}$ . The DNA affinity matrix was washed three times with binding buffer, and bound proteins were eluted by boiling in SDS-PAGE sample buffer. Boiled extracts were subjected to SDS-PAGE and Western blotting.

**In Vitro and in Vivo SUMO Conjugation**—*In vitro* sumoylation assays performed with 2  $\mu\text{l}$  of *in vitro* translated wtFLI-1 protein in reticulocyte lysate (Promega) were performed as described previously (27). To detect sumoylated FLI-1 *in vivo*,  $0.5 \times 10^6$  HeLa cells were seeded in 60-mm<sup>2</sup> Petri dishes and transfected 24 h later with  $\Delta\text{EB-HA-FLI-1}$  along with pSG5-His-SUMO-1 or pSG5-His-HA-SUMO-2 as indicated. After 48 h, cells were washed twice with ice-cold PBS and lysed in 1 ml of 6 M guanidinium chloride, 0.1 M NaH<sub>2</sub>PO<sub>4</sub>, and 10 mM Tris-HCl (pH 8.0), and 50  $\mu\text{l}$  of lysate was precipitated with 1 ml of 5% trichloroacetic acid for 2 h at room temperature. After centrifugation at 15,000 rpm for 30 min, the trichloroacetic acid protein precipitates were rinsed two times with acetone, air-dried, resuspended in 20  $\mu\text{l}$  of SDS-PAGE sample buffer, and subjected to SDS-PAGE and Western blotting. To

## FLI-1 Functionally Interacts with PIAS $\alpha$

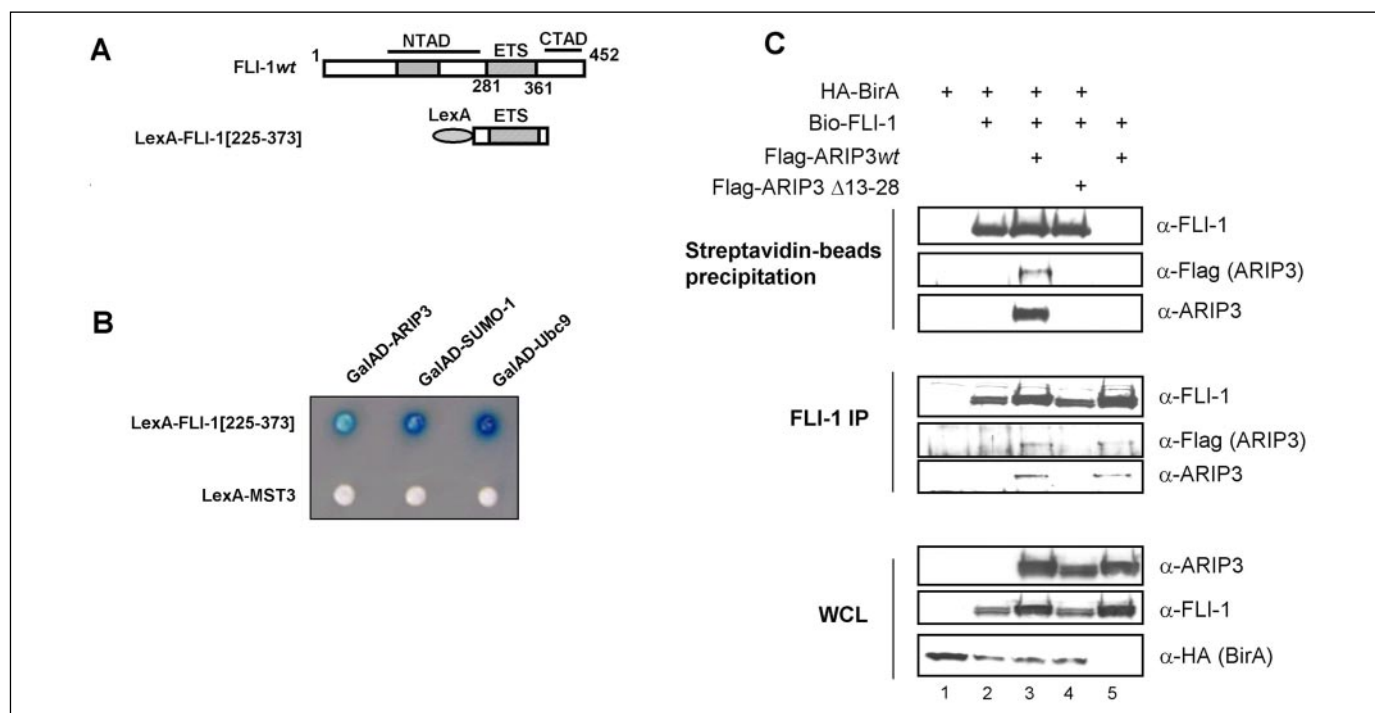


**FIGURE 1. Schematic diagram of the FLI-1 protein and the interaction of FLI-1 and PIAS $\alpha$ .** *A*, shown is a diagram of the FLI-1 functional domains. The ETS domain is shown as a hatched box, and the pointed/SAM domain as a gray box. NTAD, N-terminal activation domain; CTAD, C-terminal activation domain. The LexA fusion protein encompassing amino acids 225–373 of FLI-1, used as bait in the yeast two-hybrid screen, is depicted. LexA-MST3 (full-length) was used as a negative control. *B*, transformants were assayed for  $\beta$ -galactosidase activity and analyzed by LacZ staining. *C*, 293 cells were transfected with combinations of expression plasmids encoding the indicated proteins. Biotagged FLI-1 (*Bio-FLI-1*) was isolated by affinity chromatography using streptavidin beads (*upper panels*) or by immunoprecipitation (IP) using anti-FLI-1 antibody (*middle panels*) as described under “Experimental Procedures,” and blots were processed for Western analyses using anti-FLAG, anti-ARIP3, or anti-FLI-1 antibody to detect FLAG-ARIP3 and FLI-1. Whole cell lysates (WCL) used in the immunoprecipitation and affinity chromatography analyses were subjected to SDS-PAGE and processed for Western blotting using anti-ARIP3, anti-FLI-1, or anti-HA antibody to confirm expression and input of the respective proteins (*lower panels*).

detect ARIP3-mediated FLI-1 sumoylation *in vivo*,  $0.5 \times 10^6$  293 cells were seeded in 60-mm<sup>2</sup> Petri dishes and transfected with  $\Delta$ EB-HA-wtFLI-1 together with pSG5-His-SUMO-1 and/or pFLAG-wtARIP3 when appropriate. After 48 h, the cells were washed twice with ice-cold PBS and lysed directly in 200  $\mu$ l of SDS-PAGE sample buffer. Lysates were sonicated for 20 s on ice at low intensity to fragment genomic DNA, and 20  $\mu$ l was subjected to SDS-PAGE and Western blotting.

## RESULTS

**Isolation of the SUMO Ligase PIAS $\alpha$  as a Binding Partner of FLI-1 in a Yeast Two-hybrid Screen**—In a search for potential partners of FLI-1, a yeast two-hybrid screen of a human bone marrow cDNA library was performed using, as bait, a fusion between the LexA DNA-binding domain and amino acids 225–373 of FLI-1 (LexA-FLI-1-(225–373)). This region includes a domain unique to the FLI-1/ERG subfamily of ETS proteins (residues 257–276) as well as the entire ETS domain (Fig. 1A). Three interactors involved in the post-translational modification of proteins by SUMO, including SUMO-1 itself, Ubc9, and PIAS $\alpha$ , were identified as positive clones in this screen. These interactions were specific because coexpression of LexA-FLI-1-(225–373) with Gal4AD-PIAS $\alpha$ , Gal4AD-SUMO-1, or Gal4AD-Ubc9 activated the *lacZ* reporter present in the indicator yeast strain, whereas the control LexA-MST3 bait failed to interact with any of these Gal4AD fusion proteins (Fig. 1B). Of note, LexA-FLI-1-(225–373) did not auto-activate the *lacZ* reporter (data not shown).

To analyze whether FLI-1 and PIAS $\alpha$  interact *in vivo*, 293 cells were cotransfected with expression vectors encoding a FLAG-tagged version of rat PIAS $\alpha$  (also known as ARIP3) (18), FLI-1, and the *Escherichia coli* BirA biotin ligase. The FLI-1 protein used in this study was tagged at its

N-terminal end with a 23-amino acid peptide selected as a highly specific biotinylation substrate for *E. coli* BirA through iterative screening of combinatorial libraries (Ref. 28 and references therein). Under these conditions, biotagged FLI-1 was efficiently biotinylated by BirA (data not shown), allowing its rapid and essentially quantitative purification from cell extracts by affinity chromatography on a streptavidin affinity matrix. As shown in Fig. 1C, coexpression of biotagged FLI-1, ARIP3, and BirA resulted in the co-purification of ARIP3 and affinity-purified FLI-1 as detected by Western blot analyses using antibody to either FLAG or ARIP3 (Fig. 1C, *upper panels*, lane 3). No such co-purification was detected when the BirA expression plasmid was omitted from the cotransfection mixture (Fig. 1C, *upper panels*, lane 5). The interaction between FLI-1 and ARIP3 was also observed using anti-FLI-1 antibody in a conventional co-immunoprecipitation assay (Fig. 1C, *middle panels*).

**ARIP3 Interacts *in Vivo* with FLI-1 in a SAP Domain-dependent Fashion**—To identify the domains of ARIP3 that are involved in its ability to associate with FLI-1, we compared the ability of a series of ARIP3 deletion mutants (Fig. 2A) and wtARIP3 to interact with FLI-1. As shown in Fig. 2B, ARIP3-( $\Delta$ 102–207), ARIP3-( $\Delta$ 198–337), and SUMO ligase-deficient ARIP3-( $\Delta$ 347–418) and ARIP3-( $\Delta$ 346–475) co-purified with FLI-1. This shows that most of the N-terminal domain and the zinc finger domain of ARIP3 are not essential for this interaction. In sharp contrast, disruption of the ARIP3 SAP domain by deletion of amino acids 13–28 (ARIP3-( $\Delta$ 13–28)) abolished the ability of ARIP3 to interact with FLI-1 as analyzed by either affinity purification or co-immunoprecipitation (Figs. 1C and 2B).

The C-terminal part of FLI-1 (amino acids 225–373) was sufficient for its interaction with ARIP3 in the yeast two-hybrid experiments. This

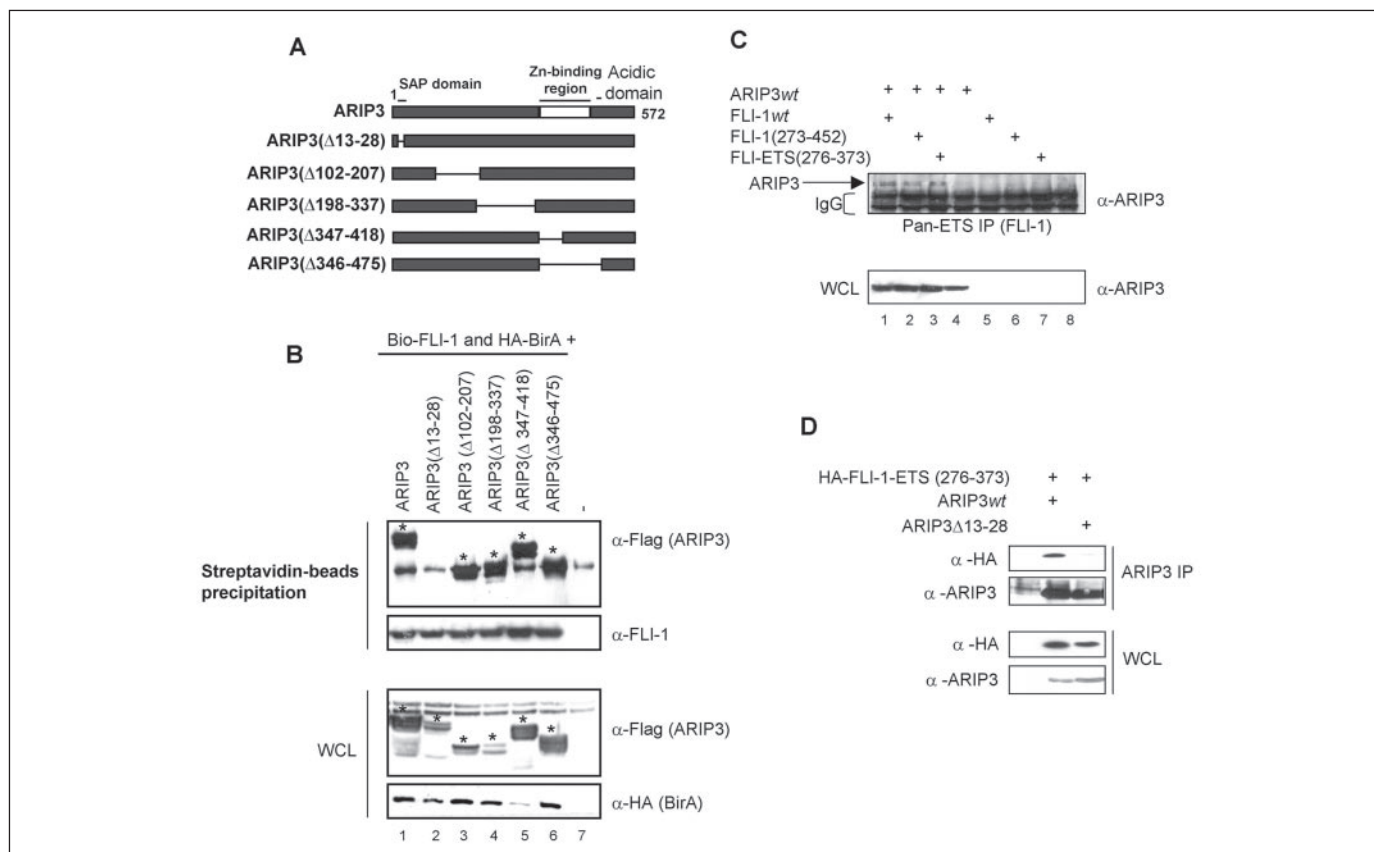


**FIGURE 2. The interaction between FLI-1 and ARIP3 depends on the ETS domain of FLI-1 and the integrity of the SAP domain of ARIP3.** *A*, shown is a schematic representation of the different N-terminally FLAG-tagged ARIP3 deletion mutants used in this study. *B*, 293 cells were transfected with expression vectors encoding the indicated proteins. FLI-1 was isolated by affinity chromatography using streptavidin beads; the isolated proteins were subjected to SDS-PAGE; and the gels were processed for Western blotting (*upper panels*). Blots were stained with anti-FLAG (to detect FLAG-tagged ARIP3) and anti-FLI-1 antibodies. The whole cell lysate (*WCL*) used for the affinity chromatography purification was analyzed to confirm expression of the different ARIP3 mutants (anti-FLAG antibody) and of BirA (anti-HA antibody) (*lower panels*). The asterisks indicate wtARIP3 and mutants derived thereof. *Bio-FLI-1*, biotagged FLI-1. *C*, 293 cells were transfected with expression vectors encoding the indicated proteins. FLI-1 mutants were immunoprecipitated (*IP*) using anti-pan ETS antibody (which recognizes the ETS domain), and the immunoprecipitates were subjected to SDS-PAGE and Western blotting. Blots were analyzed for the presence of ARIP3 in the FLI-1 precipitates using anti-ARIP3 antibody (*upper panel*). The whole cell lysate used for the immunoprecipitation was analyzed by Western blotting to confirm the expression of ARIP3 using anti-ARIP3 antibody (*lower panel*). *D*, 293 cells were transfected with expression vectors encoding the indicated proteins. ARIP3 was immunoprecipitated using anti-ARIP3 antibody, and immunoprecipitates (*upper panels*) as well as whole cell lysates (*lower panels*) were subjected to SDS-PAGE and Western blotting. Blots were stained with the indicated antibodies.

region of FLI-1 includes the entire ETS domain (amino acids 277–361) and an upstream region conserved in the FLI-1/ERG subfamily of ETS proteins. Besides its specific interaction with DNA, the ETS domain mediates interactions with a number of proteins, including GATA-1 (6) and erythroid-specific Krüppel-like factor (10). We next analyzed whether this region of FLI-1 is involved in the interaction with ARIP3 *in vivo*. As is apparent in Fig. 2C, wtFLI-1 and its isolated ETS domain (FLI-1-(276–373)) were equally efficient in co-immunoprecipitating ARIP3, showing that the ETS domain is sufficient to mediate the interaction with ARIP3. This interaction was specific, as the antibody directed against the ETS domain of FLI-1 did not coprecipitate ARIP3 when the wtFLI-1 or FLI-1-(276–373) expression vector was omitted from the transfection mixture (Fig. 2C, lane 4). Similar to wtFLI-1, the interaction of the ETS domain (FLI-1-(276–373)) with ARIP3 depended upon the integrity of the SAP domain, as the ETS domain failed to coprecipitate with ARIP3-( $\Delta$ 13–28) (Fig. 2D). We conclude from these experiments that FLI-1 specifically interacts with ARIP3 *in vivo* and that this interaction involves the ETS domain of FLI-1 and requires the integrity of the SAP domain of ARIP3.

*The Interaction between FLI-1 and ARIP3 Is Direct and Does Not Require Cofactors*—To analyze whether the interaction between FLI-1 and ARIP3 is direct, we next performed GST pull-down experiments using, as affinity matrices, a series of GST fusion proteins corresponding

to specific functional domains of FLI-1 (Fig. 3A). Full-length wtARIP3 and a series of ARIP3 deletion mutants were synthesized as radiolabeled proteins by *in vitro* translation, and their association with the different GST-FLI-1 fusion proteins and control GST was compared. As shown in Fig. 3B, GST-FLI-1-(3–208) and GST-FLI-1-(3–286), which encompass the N-terminal half of FLI-1, including its pointed/SAM domain, failed to pull down ARIP3. In contrast, both GST-FLI-1-(188–452) and GST-FLI-1-(250–452), which span the C-terminal part of FLI-1, including its ETS domain, specifically bound ARIP3. In line with the results obtained *in vivo*, disruption of the SAP domain in ARIP3-( $\Delta$ 13–28) inhibited the ability of ARIP3 to interact with GST-FLI-1-(250–452) (Fig. 3C). In contrast, deletion of amino acids 102–207 and 198–337 in the N-terminal half of the protein and the zinc finger domain (ARIP3-(347–418)) and downstream sequences (ARIP3-(346–475)) did not affect ARIP3 binding to FLI-1. PIAS $\alpha$  is expressed in two isoforms, PIAS $\alpha$  and PIAS $\beta$ , which differ only at their extreme C-terminal ends. As expected from the results obtained with PIAS $\alpha$ /ARIP3, PIAS $\beta$  was coprecipitated as efficiently as ARIP3 by GST-FLI-1-(250–452) (Fig. 3C).

*ARIP3 and PIAS $\beta$  Stimulate FLI-1 Sumoylation In Vitro*—Ubc9 and PIAS $\alpha$ /ARIP3 are critical components of the SUMO modification pathway of proteins, in which Ubc9 is the E2 conjugating enzyme, whereas PIAS $\alpha$ /ARIP3 and other PIAS family members are E3 ligases

## FLI-1 Functionally Interacts with PIAS $\alpha$

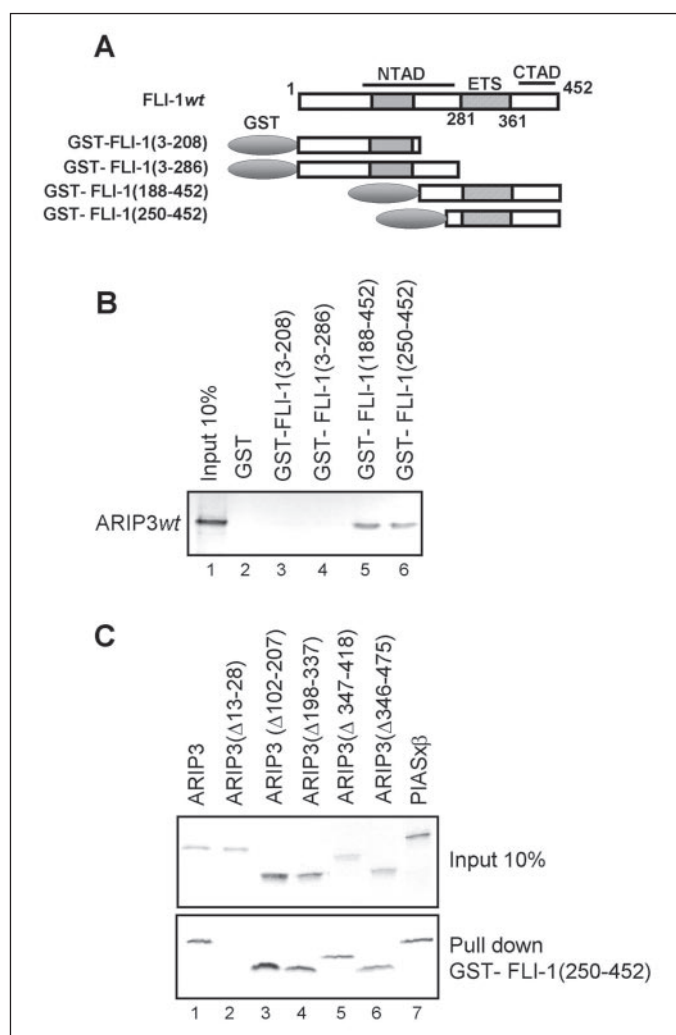


**FIGURE 3. ARIP3 and FLI-1 interact directly *in vitro*.** *A*, shown is a schematic representation of the different FLI-1 deletion mutants fused to GST used in this study. The ETS domain is shown as a *hatched box*; the pointed/SAM domain is shown as a *gray box*; and the GST domain is shown as a *gray oval*. NTAD, N-terminal transcriptional activation domain; CTAD, C-terminal transcriptional activation domain. *B* and *C*, GST-FLI-1 deletion mutants were isolated from transformed and isopropyl  $\beta$ -D-thiogalactopyranoside-induced bacteria, purified on glutathione-agarose beads, and incubated with *in vitro* transcribed/translated [ $^{35}$ S]methionine/cysteine-labeled wtARIP3 (*B*) or the indicated deletion mutants of ARIP3 (*C*). GST pull-down assays were performed as described under "Experimental Procedures," and bound proteins were subjected to SDS-PAGE, followed by fluorography of the dried gel.

that facilitate SUMO conjugation to specific substrates (17). Because FLI-1 interacts physically with both Ubc9 and ARIP3, we next examined whether FLI-1 can be sumoylated *in vitro* and whether its sumoylation can be enhanced by PIAS proteins. L-[ $^{35}$ S]Methionine/cysteine-labeled HA-tagged wtFLI-1 produced by *in vitro* translation was incubated in the presence of ATP and a cellular fraction containing SUMO E1-activating activity together with recombinant Ubc9 and SUMO-1 in the absence or presence of recombinant PIAS proteins. As expected, translation of the *FLI-1* mRNA occurred both at the initiator methionine and at a second translation initiation AUG codon at position 34 (Fig. 4A, lane 1). In the presence of SUMO-1, two slow migrating forms were additionally observed, corresponding to the expected increase in apparent molecular mass resulting from addition of a single SUMO-1 adduct to each of the FLI-1 variants. Addition of PIAS3 or PIASy had no detectable effect on FLI-1 sumoylation levels, whereas PIAS1 clearly enhanced FLI-1 sumoylation (Fig. 4A). In contrast, addition of either PIAS $\alpha$  or PIAS $\beta$  strongly enhanced FLI-1 sumoylation and resulted in the

appearance of FLI-1 forms that most likely correspond to the conjugation of several SUMO adducts (Fig. 4A, lanes 5 and 6). These results show that FLI-1 can be conjugated to SUMO-1 *in vitro* and that this modification is significantly enhanced by specific members of the PIAS family of SUMO ligases.

*Lysine 67 Is the Major SUMO Modification Site in FLI-1 in Vivo*—Next, we investigated whether FLI-1 is sumoylated *in vivo*. Expression vectors encoding HA-tagged wtFLI-1 and either His-tagged SUMO-1 or His-HA-tagged SUMO-2 were transiently transfected into HeLa cells, followed by lysis in a guanidinium chloride-containing buffer (see "Experimental Procedures"), and whole cell extracts were analyzed by Western blotting using anti-FLI-1 antibody. HA-tagged FLI-1 migrates as a major species of 50 kDa and a minor component resulting from internal initiation at Met<sup>34</sup>. In the presence of exogenous SUMO-1 or SUMO-2, slow migrating forms of FLI-1 were observed with an increase in apparent molecular mass corresponding to monosumoylation (Fig. 4B, lanes 3 and 4). Of note, a band migrating below the exogenous SUMO-1- and SUMO-2-FLI-1 adducts was present in lanes 2–4 and likely represents FLI-1 sumoylation with endogenous SUMO. Protein sumoylation often targets lysine residues in a  $\phi$ KXE consensus sequence, where K corresponds to the lysine residue to which SUMO-1 is covalently bound,  $\phi$  to a hydrophobic amino acid, and X to any amino acid. Perfect or near perfect matches to this motif are found in FLI-1 around Lys<sup>67</sup> and Lys<sup>217</sup>, both localized in the N-terminal half of the protein. To investigate whether these residues are *in vivo* acceptor sites for SUMO-1 or SUMO-2, they were mutated either singly or in combination to non-sumoylatable arginine to generate FLI-1-(K67R), FLI-1(K217R), and FLI-1-(K67R,K217R), respectively. Sumoylation of these mutants was compared with that of wtFLI-1 following transient transfection of the corresponding expression plasmids together with the expression plasmid for either SUMO-1 or SUMO-2. As shown in Fig. 4C, FLI-1(K217R) was modified as efficiently as wtFLI-1. In contrast, mutation of Lys<sup>67</sup> in FLI-1(K67R) and FLI-1(K67R,K217R) abolished the formation of the retarded sumoylated form of FLI-1. These results show that FLI-1 is sumoylated *in vivo* at a single lysine residue (Lys<sup>67</sup>) located in its N-terminal domain and that both SUMO-1 and SUMO-2 can serve as substrates for this modification. Of note, the higher migrating forms of FLI-1 *in vitro*, presumably corresponding to multisumoylation of FLI-1, were not observed *in vivo*. Next, we studied whether ARIP3 is able to enhance sumoylation of FLI-1 *in vivo*. Fig. 4D shows that coexpression of FLI-1 with ARIP3 enhanced sumoylation of FLI-1 *in vivo*, using endogenous SUMO as a substrate (Fig. 4D, compare lanes 1 and 4). Coexpression of HA-tagged SUMO-1 together with FLI-1 resulted in a second, slower migrating form of FLI-1 (corresponding to the covalent attachment of HA-tagged SUMO-1), which was enhanced by coexpression with ARIP3 (Fig. 4D, compare lanes 2 and 4). These experiments indicate that FLI-1 is sumoylated at Lys<sup>67</sup> and that ARIP3 functions as a SUMO ligase for FLI-1 *in vitro* and *in vivo*.

*ARIP3 Interferes with FLI-1 Transcriptional Activity*—PIAS $\alpha$ /ARIP3 was originally characterized as an androgen receptor-interacting protein that functions as a co-regulator of the androgen receptor and other members of the nuclear hormone receptor family (18). PIAS $\alpha$ /ARIP3 was later shown to enhance sumoylation of cell proteins, and its SUMO ligase activity can be critical for PIAS $\alpha$ /ARIP3 to regulate transcription (24, 29). We therefore analyzed whether ARIP3 is able to modulate the transcriptional regulatory activity of FLI-1. Increasing amounts of the expression vector encoding ARIP3 were cotransfected together with fixed amounts of the FLI-1 expression plasmid and the EBS-driven luciferase reporter gene. Transactivation was monitored by luciferase activity assay. Consistent with previous results (13), FLI-1

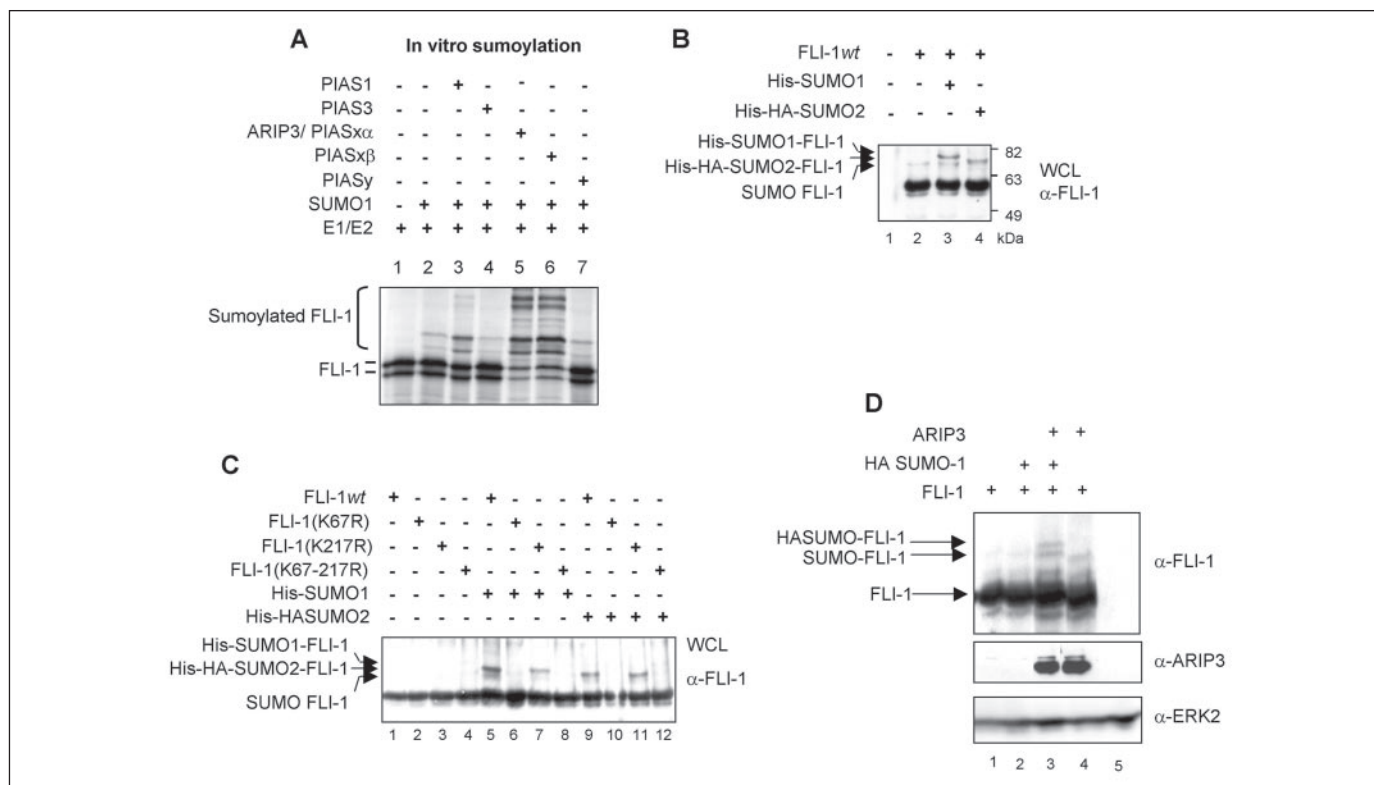


**FIGURE 4. FLI-1 is a SUMO substrate of specific PIAS family members *in vitro* and is sumoylated *in vivo*.** A, recombinant proteins of different members of the PIAS family, HeLa cell extract containing SUMO E1-activating activity, and recombinant E2 (Ubc9) and SUMO-1 were incubated with *in vitro* transcribed/translated [<sup>35</sup>S]methionine/cysteine-labeled wtFLI-1 for 1 h. Reaction contents were subjected to SDS-PAGE and fluorography of the dried gel to visualize the sumoylation pattern of FLI-1. FLI-1 migrates as a doublet due to a natural occurring alternative translation initiation site at AUG encoding Met<sup>34</sup>. B and C, HeLa cells were transfected with combinations of expression vectors encoding the indicated proteins; cells were lysed; and whole cell lysates (WCL) were insolubilized with trichloroacetic acid, resuspended in SDS-PAGE sample buffer, subjected to SDS-PAGE, and processed for Western blotting using anti-FLI-1 antibody. D, 293 cells were transfected with combinations of expression vectors encoding the indicated proteins; cells were lysed as described under "Experimental Procedures"; and whole cell protein extracts were subjected to SDS-PAGE and Western blotting. The blot was successively stained with anti-FLI-1 (*upper panel*), anti-ARIP3 (*middle panel*), and anti-ERK2 (loading control; *lower panel*) antibodies. Arrows indicate the presence of wtFLI-1 and sumoylated FLI-1 adducts.

efficiently activated luciferase expression from tkD2A-Luc, a luciferase reporter gene in which a tandem copy of ETS-responsive region-1 of the human T-cell leukemia virus type I long terminal repeat is inserted upstream of the -55 herpes simplex virus thymidine kinase promoter (Fig. 5A). Increasing amounts of ARIP3 inhibited FLI-1-mediated transactivation of tkD2A-Luc in a dose-dependent manner (Fig. 5A). The inhibitory action of ARIP3 on FLI-1-mediated transactivation are not restricted to model promoters because ARIP3 also efficiently and specifically inhibited the EBS-dependent (30), FLI-1-mediated transactivation of the *mfl-1*(-270/-41) gene promoter (Fig. 5A, *upper right panel*). Notably, ARIP3 did not affect the basal activity of either tkD2A-Luc or *mfl-1*(-270/-41)-Luc, and it did not affect FLI-1 expression (Fig. 5A, *lower panels*).

*Neither the Sumoylation of FLI-1 at Lys<sup>67</sup> nor the Ligase Activity of ARIP3 Is Essential for ARIP3 to Function as a Repressor of FLI-1 Transactivation*—To determine whether ARIP3 repressive function depends upon FLI-1 sumoylation, we compared the ability of ARIP3 to inhibit wtFLI-1 and the sumoylation-defective FLI-1(K67R) mutant. As shown in Fig. 5B, transactivation of the *mfl-1*(-270/-41)-Luc reporter gene by FLI-1(K67R) was similar to that induced by wtFLI-1 (Fig. 5B), indicating that the K67R mutation is without effect on FLI-1 transactivation properties. Of note, the DNA-binding ability of FLI-1(K67R) as assayed by electrophoretic mobility shift assay was similar to that of wtFLI-1 (data not shown). In addition, transactivation by wtFLI-1 or FLI-1(K67R) was similarly impaired in the presence of increasing amounts of ARIP3 (Fig. 5C), indicating that mutation of Lys<sup>67</sup> and therefore FLI-1 sumoylation are not required for ARIP3-mediated repression of FLI-1

transcriptional activity. Similar results were obtained using FLI-1(K67R,K217R) and tkD2A-Luc instead of *mfl-1*(-270/-41)-Luc as the reporter gene construct (data not shown). We next examined whether the SUMO ligase activity of ARIP3 is required to inhibit FLI-1 transcriptional regulatory properties. To this end, we compared the inhibitory activity of wtARIP3 and either an ARIP3 mutant with a RING finger region deletion (ARIP3-( $\Delta$ 347-418)) or a mutant in which a tryptophan residue conserved in the RING zinc finger of ARIP3 was changed to alanine (ARIP3(W383A)). Previous analyses have shown that both these mutations impair ARIP3 E3 activity (24). As shown in Fig. 5D, both ARIP3-( $\Delta$ 347-418) and ARIP3(W383A) inhibited FLI-1-mediated transcriptional activation of *mfl-1*(-270/-41)-Luc in a manner indistinguishable from wtARIP3. Taken together, these results show that the ARIP3 inhibitory action on FLI-1-induced transactivation requires neither the SUMO ligase activity of ARIP3 nor FLI-1 sumoylation. Notably, although PIASx $\beta$  was able to sumoylate and interact with FLI-1 *in vitro*, no repressive effect of PIASx $\beta$  on FLI-1 transactivation could be observed under these experimental conditions (data not shown).

*ARIP3 Relocalizes FLI-1 to Nuclear Bodies*—PIAS proteins localize to specific nuclear bodies of unclear composition and function that are detected as punctate structures by confocal immunofluorescence microscopy (23, 31, 32). To examine whether ARIP3 can change FLI-1 subnuclear localization, indirect two-color immunofluorescence was performed in cells expressing either wtFLI-1 or ARIP3 alone or together. As shown in Fig. 6A, single-plane microscopy revealed an essentially diffuse nuclear pattern for FLI-1 when expressed alone. In

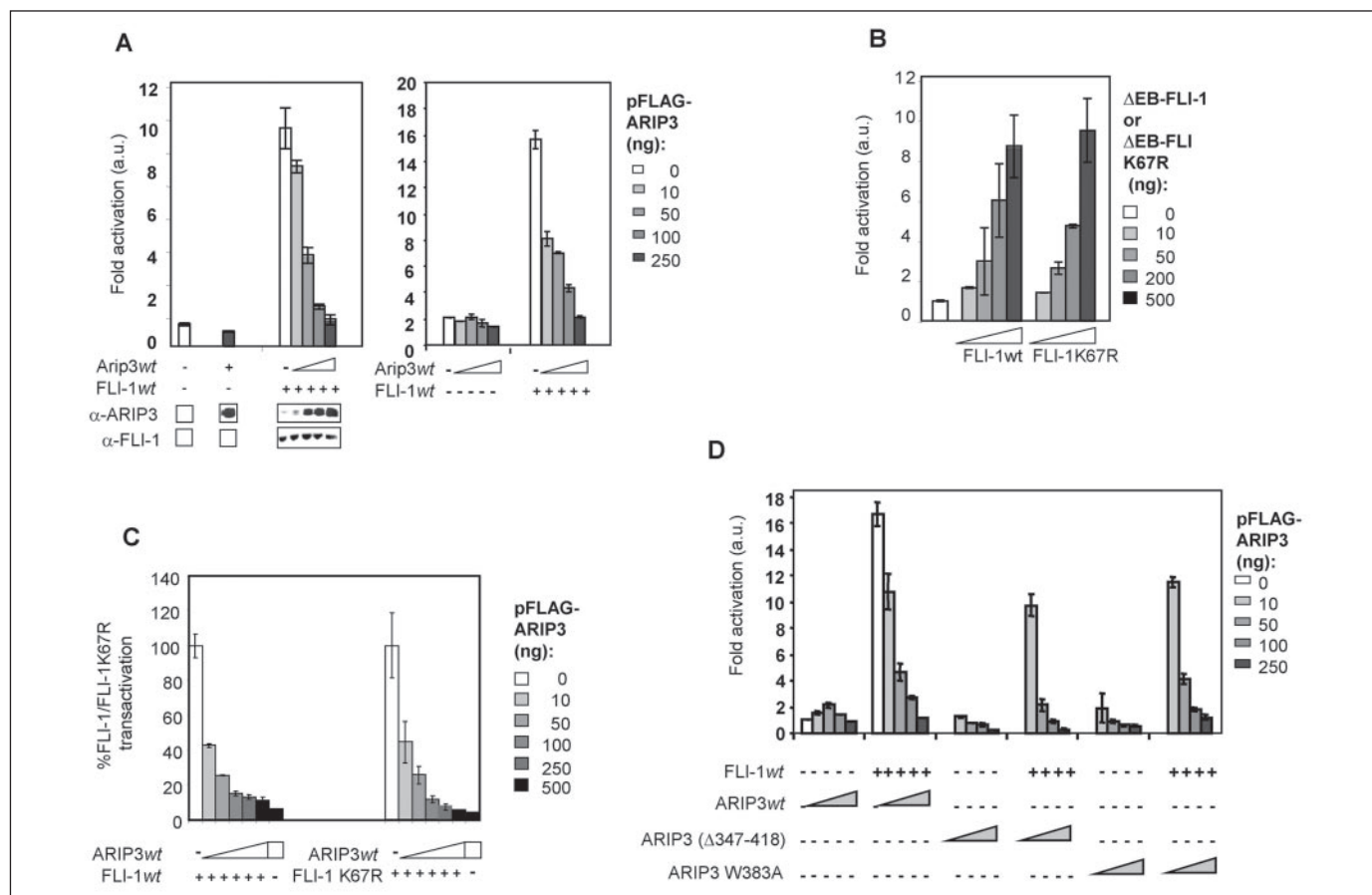


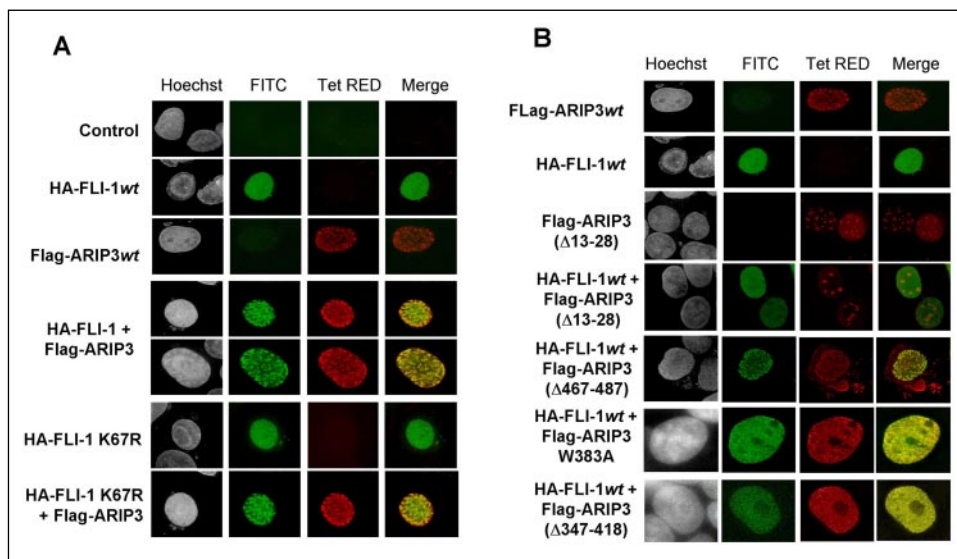
**FIGURE 5. ARIP3 represses FLI-1-induced transactivation.** *A*, 293 cells were transfected with 600 ng of tkD2A-Luc (upper left panel) or mFlI-1(-270/-41)-Luc (upper right panel) reporter gene together with 150 ng of FLI-1 and increasing amounts of ARIP3 as indicated. Cells were lysed after 24 h, and extracts were assayed for luciferase activity. The lower panels represent the whole cell lysate subjected to SDS-PAGE and Western blotting to verify the expression of FLI-1 using anti-FLI-1 antibody and increasing amounts of ARIP3 using anti-ARIP3 antibody. *Error bars* represent the S.D. of at least three independent experiments. *B*, 293 cells were transfected with the tkD2A-Luc reporter gene together with the indicated amounts of expression plasmid encoding either wtFLI-1 or the sumoylation-defective FLI-1(K67R) mutant. *C*, 293 cells were transfected with the tkD2A-Luc reporter gene (600 ng) together with a fixed amount (150 ng) of FLI-1 expression vector with or without the indicated amounts of the ARIP3 expression plasmid. Cells were harvested 24 h after transfection, and luciferase content was assessed as described under "Experimental Procedures." The effect of ARIP3 on FLI-1 transactivation is shown relative to FLI-1 or FLI-1(K67R) transactivation without ARIP3, which was put at 100%. *Error bars* represent the S.D. of at least three independent experiments. *D*, 293 cells were transfected with the tkD2A-Luc reporter gene together with the expression plasmid for wtFLI-1 and increasing amounts of wtARIP3, ARIP3( $\Delta$ 347-418), or ARIP3(W383A) as indicated. Cells were harvested 24 h after transfection, and luciferase activity in cell extracts was assessed as described under "Experimental Procedures." *Error bars* represent the S.D. of at least three independent experiments. In *A-C*, fold activation was calculated as the increase in luciferase activity induced by coexpressed FLI-1 and ARIP3 proteins compared with basal reporter gene activity. *a.u.*, arbitrary units.

contrast, ARIP3 localized to nuclear speckles (Fig. 6A), in agreement with previous studies (23). Similar results were obtained in HeLa cells (data not shown). Strikingly, coexpression of ARIP3 and FLI-1 led to a partial relocalization of FLI-1 to ARIP3 nuclear bodies (Fig. 6A). Relocalization is independent of FLI-1 sumoylation, as the non-sumoylatable FLI-1(K67R) mutant also relocalized to ARIP3 nuclear bodies upon coexpression with ARIP3 (Fig. 6A). Because an intact SAP domain in ARIP3 is essential for its ability to interact physically with FLI-1, we analyzed the ability of ARIP3( $\Delta$ 13-28) to relocalize FLI-1. Interestingly, ARIP3( $\Delta$ 13-28) displayed a different pattern of nuclear body formation compared with wtARIP3, forming a small number of larger structures (2-15/nucleus) (Fig. 6B). Unlike wtARIP3, ARIP3( $\Delta$ 13-28) failed to relocalize FLI-1 to nuclear bodies, indicating that the integrity of the SAP domain is essential to the ability of ARIP3 to sequester FLI-1 into nuclear bodies (Fig. 6B). Deletion of amino acids 467-487 (the SUMO-binding region of ARIP3), which leads to the formation of fewer nuclear dots (23) and to partial cytoplasmic localization of ARIP3, also relocalized FLI-1 to nuclear dots (Fig. 6B). This indicates that relocalization of FLI-1 to ARIP3 nuclear bodies is independent of SUMO binding to ARIP3. As described previously for ARIP3 and other PIAS family

members (23, 31), E3-deficient mutants of ARIP3, *viz.* ARIP3( $\Delta$ 347-418) and ARIP3(W383A), displayed a diffuse nuclear localization. Coexpression of FLI-1 with either ARIP3( $\Delta$ 347-418) or ARIP3(W383A) did not change the diffuse pattern normally seen with FLI-1 (Fig. 6B). Because these mutants efficiently bound FLI-1 and repressed FLI-1 transcriptional activation properties, ARIP3-mediated relocalization of FLI-1 to nuclear bodies does not seem to be sufficient to explain its ability to functionally repress FLI-1.

**ARIP3 Does Not Inhibit FLI-1 DNA-binding Activity**—The mapping studies described above indicated that the ETS domain of FLI-1 is sufficient to interact physically with ARIP3. It is therefore possible that the inhibitory properties of ARIP3 result from its ability to impair the DNA-binding activity of FLI-1 for EBS sequences. The specific DNA-binding activity of FLI-1 for an optimal EBS oligonucleotide was not inhibited when performed in the presence of excess recombinant ARIP3, as analyzed by electrophoretic mobility shift assay (data not shown). To further demonstrate that the binding of FLI-1 is compatible with complex formation with ARIP3, the specific DNA-binding activity of FLI-1 was assayed by oligonucleotide pull-down assay using a biotinylated double-stranded EBS oligonucleotide immobilized on streptavidin beads and

**FIGURE 6. FLI-1 relocates to ARIP3 nuclear bodies.** *A* and *B*, 293 cells grown on coverslips were transfected with expression plasmids encoding the indicated proteins. 48 h after transfection, cells were fixed with paraformaldehyde and stained with anti-FLI-1 antibody/fluorescein isothiocyanate (FITC)-conjugated anti-rabbit IgG to detect FLI-1 (green), anti-FLAG antibody/Texas Red (Tet RED)-coupled anti-rabbit IgG to detect ARIP3 (red), or Hoechst dye as described under "Experimental Procedures." Images were obtained as described under "Experimental Procedures," and merged image overlaps were obtained using MetaMorph software. Additional processing of images was performed using Adobe Photoshop software.



cell extracts in which HA-FLI-1 was expressed in the presence or absence of HA-ARIP3 (Fig. 7A). FLI-1 was efficiently bound by the EBS oligonucleotide affinity matrix as analyzed by Western blotting (Fig. 7B, lane 2). This binding was specific because DNA binding by FLI-1 was not observed using streptavidin beads loaded with a mutated EBS oligonucleotide as an affinity matrix (Fig. 7B, lanes 2 and 5). Notably, in extracts coexpressing HA-FLI-1 and HA-ARIP3, HA-ARIP3 was also specifically recovered from the wtEBS affinity matrix, showing that formation of the FLI-1-ARIP3 complex did not interfere with the DNA-binding activity of FLI-1 (Fig. 7B, lanes 2 and 6).

**The Interaction between FLI-1 and ARIP3 Is Essential for the Repressive Function of ARIP3 in FLI-1 Transactivation**—To analyze whether the inhibitory properties of ARIP3 are linked to its ability to physically interact with FLI-1, we analyzed the effect of a series of ARIP3 deletion mutants that either maintained or did not maintain their ability to interact with FLI-1 (Fig. 2) (data not shown) on FLI-1-mediated transactivation. Fig. 8A shows that the SAP domain of ARIP3, which is required for the physical interaction between FLI-1 and ARIP3, is also critical for the transcriptional inhibitory properties of ARIP3 because both ARIP3-( $\Delta$ 1–102) and ARIP3-( $\Delta$ 13–28) failed to inhibit FLI-1 transactivation properties. In contrast, ARIP3-( $\Delta$ 102–207), ARIP3-( $\Delta$ 102–260), ARIP3-( $\Delta$ 198–337), and ARIP3-( $\Delta$ 467–547), which associated with FLI-1 *in vivo* and *in vitro*, also fully inhibited FLI-1-mediated transactivation. Together with the data of Fig. 5D, these results show that the region of ARIP3 extending from amino acids 102 to 418 is not critical to ARIP3 inhibitory properties and that ARIP3-mediated inhibition of FLI-1 activity is linked to the ability of ARIP3 to physically bind FLI-1. Mutant ARIP3-( $\Delta$ 346–475) displayed a reduced ability to repress FLI-1. However, this protein only partially localized to the nucleus (data not shown), suggesting that the diminished inhibitory activity of this mutant is not intrinsic, but results from its incomplete accumulation in the nucleus. Of note, equal expression of FLI-1 was observed under the different conditions tested (Fig. 8B, lower panel).

## DISCUSSION

In this study, several components of the post-translational sumoylation pathway have been identified in a yeast two-hybrid screen as interactors of FLI-1, including SUMO-1 itself; Ubc9, the E2 enzyme involved in the conjugation of SUMO to the  $\epsilon$ -amino group of specific lysines in protein substrates; and PIASx $\alpha$ , one of the E3 ligases that facilitate

SUMO conjugation to specific substrates. An interaction between FLI-1 and Ubc9 has previously been reported (33), but no link was established to either FLI-1 sumoylation or regulation of FLI-1 transcriptional activity. We report here that (i) FLI-1 is sumoylated *in vitro* by recombinant Ubc9 and *in vivo* at a single lysine residue at position 67, which is part of a classical  $\phi$ KXE Ubc9-binding site located in its transcriptional activation domain; (ii) FLI-1 binds through its ETS domain to PIASx $\alpha$ , and the integrity of the SAP domain of PIASx $\alpha$  is required for this interaction; and (iii) the interaction of FLI-1 with PIASx $\alpha$  enhances FLI-1 sumoylation at Lys<sup>67</sup>, represses FLI-1 transcriptional activation properties, and leads to the sequestering of FLI-1 into PIASx $\alpha$  nuclear bodies.

PIAS proteins were first identified as repressors of the DNA-binding activity of tyrosine-phosphorylated STAT proteins, with PIAS1 and PIAS3 being specific to STAT1 and STAT3, respectively (34, 35). Later, PIASx and PIASy were shown to inhibit STAT4 and STAT1 transcriptional activity, respectively, without interfering with DNA binding (36, 37). Recent studies with *pias1*-deficient cells have shown, however, that PIAS1 interfering activity is specific to a small subset of STAT1 target genes critical to the interferon- $\beta$ - and interferon- $\gamma$ -mediated innate immune responses (38). PIAS transcriptional regulatory properties are not limited to activated STAT proteins, as they have been found to regulate positively or negatively, through ill defined mechanisms, the activity of other transcription factors, e.g. members of the nuclear receptor superfamily (for review, see Ref. 17). All members of the PIAS family have been shown to be SUMO E3 ligases that can favor sumoylation of a number of DNA-binding transcriptional regulators and co-regulators (for review, see Ref. 17). Gene inactivation of Siz1 and Siz2, the PIAS homologs in yeast, results in reduction in global protein sumoylation (39), and the *Drosophila melanogaster* PIAS homolog SU(VAR)2-10 is required for viability. In contrast, gene inactivation of PIASx, PIAS1, or PIASy by homologous recombination in mouse cells has no discernible effect on global protein sumoylation and is viable, indicating that PIAS proteins are likely to be redundant in mammals (38, 40–42). Our *in vitro* and *in vivo* experiments have shown that FLI-1 conjugation to SUMO-1 is specifically enhanced by PIASx $\alpha$ /ARIP3 and its spliced variant PIASx $\beta$ , but much less efficiently by PIAS1 and not at all by PIASy and PIAS3, indicating a clear selectivity for specific members of the PIAS family. The reduced activity of PIAS1 does not reflect a failure to interact with FLI-1 because FLI-1 and PIAS1 were found to physically

## FLI-1 Functionally Interacts with PIAS $\alpha$

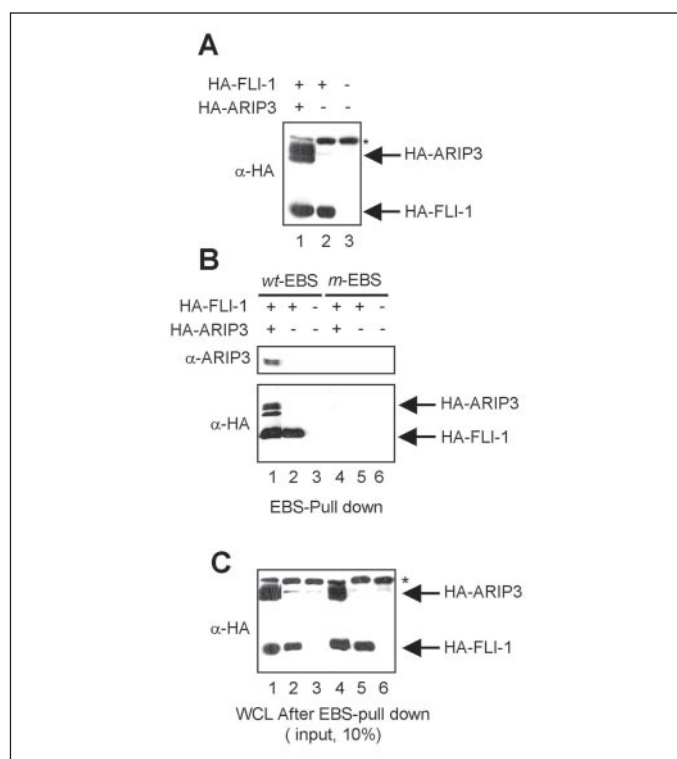


**FIGURE 7. FLI-1 binding to ETS-binding sequences is not inhibited by ARIP3.** *A*, shown are the results from expression analysis of FLI-1 and ARIP3 in the whole cell extracts used in *B*. 293 cells were transfected with vectors encoding HA-FLI-1 alone or with HA-ARIP3, lysed after 48 h as described under "Experimental Procedures," and subjected to SDS-PAGE and Western blotting. Blots were stained with anti-HA antibody to detect HA-FLI-1 and HA-ARIP3. *B*, the 293 lysates described for *A* containing FLI-1 and/or ARIP3 were subjected as indicated to oligonucleotide pull-down assay using, as an affinity matrix, either biotinylated wtEBS or mutant EBS (*m-EBS*) carrying a GG-to-CC transition in its core. Briefly, lysates were incubated with biotinylated wtEBS or mutant EBS double-stranded oligonucleotides immobilized on streptavidin beads. Bound proteins were analyzed by SDS-PAGE and Western blotting using anti-HA (*upper panel*) and anti-ARIP3 (*lower panel*) antibodies. *C*, unbound proteins in the oligonucleotide pull-down assay described for *B* were resolved by SDS-PAGE and Western blotting using anti-HA antibody to stain for HA-FLI-1 and HA-ARIP3. Both FLI-1 and ARIP3 were present in this fraction, indicating that the experiment was performed under equilibrium conditions. Arrows indicate the different proteins, and asterisks indicate the presence of a nonspecific background band. WCL, whole cell lysate.

interact when coexpressed *in vivo*,<sup>5</sup> suggesting that FLI-1 is preferentially modified by PIAS $\alpha$  proteins.

PIAS $\alpha$ /ARIP3 acts as a repressor of FLI-1-dependent EBS-driven transcription. SUMO modification of DNA-bound transcription factors often targets known repression domains and can result in enhanced repression (for review, see Ref. 17; Ref. 43). Although the SUMO target (Lys<sup>67</sup>) is located in the N-terminal activation domain of FLI-1, two lines of evidence indicate that enhanced FLI-1 sumoylation is not involved in PIAS $\alpha$ -mediated transcriptional repression. First, FLI-1(K67R), in which Lys<sup>67</sup> has been replaced with a non-sumoylatable arginine, although similarly effective in transactivation compared with wtFLI-1, was as efficiently repressed by PIAS $\alpha$ /ARIP3 as was wtFLI-1. Second, despite the fact that the closely related splice variant PIAS $\beta$  activated FLI-1 sumoylation as efficiently as PIAS $\alpha$ , it failed to inhibit FLI-1-mediated EBS-driven transcription. This situation is not unprecedented because repression of, for example, the transcriptional activity of LEF-1 by PIAS $\gamma$  is also unlinked to its PIAS $\gamma$ -mediated sumoylation at specific lysine residues (31). Interestingly, RING finger mutants of PIAS $\alpha$ /ARIP3 that are deficient in SUMO conjugation, *viz.* ARIP3(W383A) and ARIP3( $\Delta$ 347–418), fully repressed FLI-1 transactivation, indicating

<sup>5</sup> E. van den Akker, S. Ano, and J. Ghysdael, unpublished data.

that regulatory sumoylation of known FLI-1 coactivators such as p300 (13, 44) or corepressors is not critically involved in the repressive actions of PIAS $\alpha$  on FLI-1. Other transcription factors, including GATA-2 and the androgen receptor, are also repressed by PIAS family members independent of an active RING domain (45–47), but the molecular mechanisms involved remain to be characterized.

PIAS $\alpha$ /ARIP3 and other PIAS proteins are localized in nuclear bodies of largely unknown composition and function, but may partially overlap with promyelocytic leukemia nuclear bodies (23, 31). The association of PIAS proteins with nuclear bodies appears to require their SUMO ligase activity because ligase-deficient PIAS mutants are unable to assemble into PIAS bodies (31, 45). Binding of PIAS $\alpha$ /ARIP3 to other sumoylated proteins and its targeting to the nuclear matrix also seem to be required for the formation of typical PIAS $\alpha$  bodies because deletion of the SUMO-1-binding motif of PIAS $\alpha$ /ARIP3 (amino acids 467–487) and deletion of the matrix/scaffold attachment region targeting the SAP domain both impair the formation of normal PIAS $\alpha$ /ARIP3 nuclear bodies (Fig. 6) (23). Our data show that ARIP3 relocalizes the normally diffusely distributed FLI-1 protein from the nucleoplasm to PIAS $\alpha$ /ARIP3 nuclear bodies, suggesting that repression of FLI-1 could result from its relocalization to PIAS $\alpha$  bodies. However, because FLI-1 remains diffusely distributed in the nucleoplasm in cells coexpressing FLI-1 and the ligase-deficient PIAS $\alpha$ /ARIP3 mutants and because these mutants repress FLI-1-mediated transcription and interact with FLI-1 as efficiently as wtPIAS $\alpha$ , it appears that relocalization of FLI-1 to PIAS $\alpha$  nuclear bodies is not mandatory for ARIP3 to repress FLI-1 activity. However, relocalization of FLI-1 to PIAS $\alpha$ /ARIP3 nuclear bodies could stabilize the inhibitory complex. Relocalization of FLI-1 to nuclear bodies is also independent of FLI-1 sumoylation because the sumoylation-deficient FLI-1(K67R) mutant relocalized to PIAS $\alpha$  bodies when coexpressed with PIAS $\alpha$ /ARIP3 in a fashion indistinguishable from wtFLI-1. The SAP domain of PIAS proteins binds AT-rich matrix/scaffold attachment region sequences *in vitro* (31, 32), and both PIAS $\alpha$ /ARIP3 and ligase-deficient mutants of PIAS $\alpha$  have been found to associate with detergent-insoluble nuclear fractions in a manner dependent upon their SAP domain.<sup>5</sup> It is therefore possible that, although recruitment of FLI-1 to mature PIAS $\alpha$  nuclear bodies is not instrumental in its inhibition, its targeting to the nuclear matrix could be important. A proper answer to this question will require the design of SAP domain mutations that dissociate the matrix/scaffold attachment region-targeting activity of PIAS $\alpha$  from its binding activity for FLI-1.

By what mechanism does PIAS $\alpha$  repress FLI-1 transcriptional activity? The isolated ETS domain of FLI-1 is sufficient to bind PIAS $\alpha$ /ARIP3, yet PIAS $\alpha$  failed to inhibit the specific binding of FLI-1 to canonical DNA response elements *in vitro*, suggesting that inhibition does not occur at the level of DNA binding. Our mutant studies have shown that PIAS $\alpha$ -mediated repression correlates with physical complex formation between FLI-1 and PIAS $\alpha$ . A small deletion in the SAP domain of PIAS $\alpha$  suppressed both PIAS $\alpha$ /ARIP3 repressive activity and complex formation with FLI-1, whereas mutations in other domains of PIAS $\alpha$  affected neither repression nor binding to FLI-1. Complex formation between FLI-1 and PIAS $\alpha$  could result in masking of the FLI-1 activation domain, thereby competing for the recruitment of coactivators. We do not favor this notion because EWS-FLI-1-mediated EBS-dependent transactivation, which relies entirely on a structurally unrelated, EWS-derived activation domain (20), was also inhibited by PIAS $\alpha$ /ARIP3.<sup>5</sup> Previous analyses have shown that transcriptional repression of the androgen receptor by PIAS $\gamma$  and of STAT4 by PIAS $\alpha$  involves the recruitment of histone deacetylase or histone deacetylase-

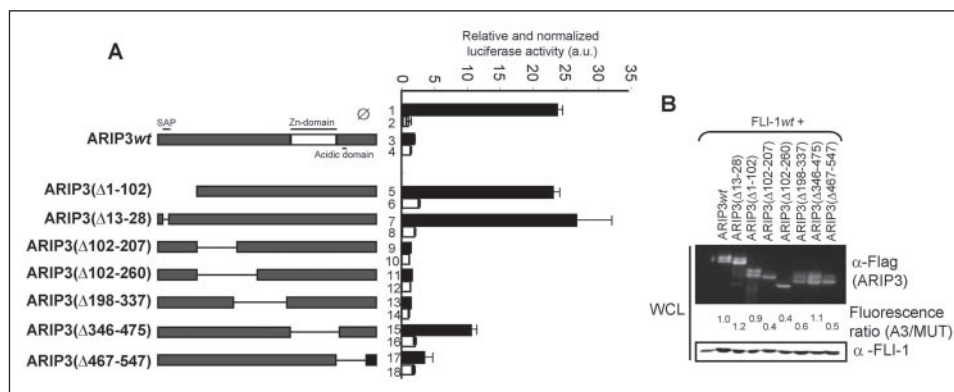


**FIGURE 8. ARIP3-induced repression of FLI-1 transactivation is dependent on the integrity of the SAP domain.** *A*, 293 cells were transfected with the tkD2A-Luc reporter gene (600 ng) and  $\Delta$ EB-FLI-1 (150 ng) in the absence (*tpo*) or presence of pFLAG-wtARIP3 (250 ng) or the indicated ARIP3 deletion mutants. The luciferase activities in the corresponding cell extracts are shown as *black bars*. The *white bars* indicate the tkD2A-Luc reporter activity when no  $\Delta$ EB-FLI-1 was present. -Fold activation was calculated as the increase in reporter gene activity compared with basal reporter gene activity (*bar 2*). To account for differences in expression levels between ARIP3 and the different mutants derived thereof, the ratio between the expression levels of wtARIP3 and its mutants was used to normalize the transactivation values (see below). *Error bars* represent the S.D. of at least three independent experiments. *B*, an aliquot of the pooled lysates from the transactivation experiment described for *A* was subjected to SDS-PAGE and Western blotting to assess the expression levels of wtARIP3 and ARIP3 deletion mutants (anti-FLAG antibody; *upper panel*) and FLI-1 (anti-FLI-1 antibody; *lower panel*) in the different samples. The expression levels were measured by quantification of luminescence using GeneSnap/GeneTools software. The relative expression ratios of the different ARIP3 mutants compared with wtARIP3 (A3/MUT) are indicated and were used to normalize the luciferase activity values. *a.u.*, arbitrary units; WCL, whole cell lysate.

associated corepressors (36, 47). We found PIASx $\alpha$ -mediated repression of FLI-1 to be insensitive to trichostatin A,<sup>5</sup> suggesting that the members of the class I and II histone deacetylase families are unlikely to be involved in PIASx $\alpha$ -mediated repression of FLI-1. PIASx $\alpha$  and PIASx $\beta$  are isoforms with similar primary amino acid sequences, except that the unique C-terminal 71 amino acids in PIASx $\alpha$  are replaced with an unrelated sequence of 122 amino acids in PIASx $\beta$ . In our experimental setting, only PIASx $\alpha$  acted as repressor for FLI-1,<sup>5</sup> suggesting either a direct role for the unique C-terminal domain of PIASx $\alpha$  in repression or an unknown role of the C-terminal domain of PIASx $\beta$  in preventing PIASx repressive activity. Experiments are in progress to compare the cofactors that associate with the repressive FLI-1·PIASx $\alpha$  complex in a manner dependent upon the unique C-terminal domain of PIASx $\alpha$ .

Our results did not identify any functional consequences of SUMO conjugation to FLI-1. It should be noted, however, that FLI-1 sumoylation occurs at low stoichiometry *in vivo* and could have functional consequences in a compartmentalized fashion. In accordance with the transportable repressive properties of SUMO-1 (45), the experimental covalent fusion of SUMO-1 to the N terminus of FLI-1 converted FLI-1 from a transcriptional activator into a repressor of EBS-mediated transcription,<sup>5</sup> suggesting that stoichiometric sumoylation of FLI-1 could be repressive. Furthermore, the functional consequences of sumoylation on several DNA-binding transcriptional regulators have been shown to depend upon the promoter context (18, 32). In this respect, like other members of the ETS family, FLI-1 functions in close synergy with other *cis*-bound DNA-binding cofactors, often on composite DNA response elements, to regulate transcriptional output. For example, in line with the requirement of FLI-1 in megakaryocytic development and differentiation (1–3), the promoters of a number of megakaryocytic lineage-specific genes contain closely juxtaposed binding sites for FLI-1 and GATA-1, a configuration that is instrumental in their developmentally regulated expression (6, 48). It is therefore possible that recruitment of the sumoylation machinery to specific promoters and sumoylation of cooperating *cis*-bound factors are important in regulating the transcriptional synergy in a promoter- and cell context-specific manner.

In conclusion, we have identified PIASx $\alpha$  as a novel repressor of FLI-1 and FLI-1-derived oncoproteins; PIASx $\alpha$  impairs FLI-1 transcriptional activity and sequesters FLI-1 into nuclear bodies. Interestingly, repression by PIASx $\alpha$  is independent of its SUMO ligase activity and of FLI-1

sumoylation, but depends upon the physical interaction between FLI-1 and PIASx $\alpha$ . The activity of FLI-1 may be repressed first through the assembly of corepressors complexes at the chromatin level and targeting of the FLI-1·PIASx $\alpha$  complex to the nuclear matrix, followed by final assembly into mature PIASx $\alpha$  nuclear bodies.

**REFERENCES**

- Hart, A., Melet, F., Grossfeld, P., Chien, K., Jones, C., Tunnacliffe, A., Favier, R., and Bernstein, A. (2000) *Immunity* **13**, 167–177
- Spyropoulos, D. D., Pharr, P. N., Lavenburg, K. R., Jackers, P., Papas, T. S., Ogawa, M., and Watson, D. K. (2000) *Mol. Cell. Biol.* **20**, 5643–5652
- Kawada, H., Ito, T., Pharr, P. N., Spyropoulos, D. D., Watson, D. K., and Ogawa, M. (2001) *Int. J. Hematol.* **73**, 463–468
- Masuya, M., Moussa, O., Abe, T., Deguchi, T., Higuchi, T., Ebihara, Y., Spyropoulos, D. D., Watson, D. K., and Ogawa, M. (2005) *Blood* **105**, 95–102
- Truong, A. H., and Ben-David, Y. (2000) *Oncogene* **19**, 6482–6489
- Eisbacher, M., Holmes, M. L., Newton, A., Hogg, P. J., Khachigian, L. M., Crossley, M., and Chong, B. H. (2003) *Mol. Cell. Biol.* **23**, 3427–3441
- Czuwara-Ladykowska, J., Shirasaki, F., Jackers, P., Watson, D. K., and Trojanowska, M. (2001) *J. Biol. Chem.* **276**, 20839–20848
- Tamir, A., Howard, J., Higgins, R. R., Li, Y. J., Berger, L., Zacksenhaus, E., Reis, M., and Ben-David, Y. (1999) *Mol. Cell. Biol.* **19**, 4452–4464
- Darby, T. G., Meissner, J. D., Ruhlmann, A., Mueller, W. H., and Scheibe, R. J. (1997) *Oncogene* **15**, 3067–3082
- Starck, J., Cohet, N., Gonnet, C., Sarrazin, S., Doubeikovska, Z., Doubeikovski, A., Verger, A., Duterque-Coquillaud, M., and Morle, F. (2003) *Mol. Cell. Biol.* **23**, 1390–1402
- Pereira, R., Quang, C. T., Lesault, I., Dolznig, H., Beug, H., and Ghysdael, J. (1999) *Oncogene* **18**, 1597–1608
- Lesault, I., Quang, C. T., Frampton, J., and Ghysdael, J. (2002) *EMBO J.* **21**, 694–703
- Ano, S., Pereira, R., Pironin, M., Lesault, I., Milley, C., Lebigot, I., Quang, C. T., and Ghysdael, J. (2004) *J. Biol. Chem.* **279**, 2993–3002
- Lebigot, I., Gardellini, P., Lefebvre, L., Beug, H., Ghysdael, J., and Quang, C. T. (2003) *Blood* **102**, 4555–4562
- Arvand, A., Welford, S. M., Teitell, M. A., and Denny, C. T. (2001) *Cancer Res.* **61**, 5311–5317
- Stein, G. S., van Wijnen, A. J., Stein, J. L., Lian, J. B., Pockwinse, S. M., and McNeil, S. (1998) *J. Cell. Biochem. Suppl.* **30–31**, 220–231
- Seeler, J. S., and Dejean, A. (2003) *Nat. Rev. Mol. Cell. Biol.* **4**, 690–699
- Moilanen, A. M., Karvonen, U., Poukka, H., Yan, W., Toppari, J., Janne, O. A., and Palvimo, J. J. (1999) *J. Biol. Chem.* **274**, 3700–3704
- Gyuris, J., Golemis, E., Chertkov, H., and Brent, R. (1993) *Cell* **75**, 791–803
- Bailly, R. A., Bosselut, R., Zucman, J., Cormier, F., Delattre, O., Roussel, M., Thomas, G., and Ghysdael, J. (1994) *Mol. Cell. Biol.* **14**, 3230–3241
- Rabault, B., and Ghysdael, J. (1994) *J. Biol. Chem.* **269**, 28143–28151
- Muller, S., Berger, M., Lehembre, F., Seeler, J. S., Haupt, Y., and Dejean, A. (2000) *J. Biol. Chem.* **275**, 13321–13329

## FLI-1 Functionally Interacts with PIASx $\alpha$

23. Kotaja, N., Karvonen, U., Janne, O. A., and Palvimo, J. J. (2002) *Mol. Cell. Biol.* **22**, 5222–5234
24. Kotaja, N., Vihinen, M., Palvimo, J. J., and Janne, O. A. (2002) *J. Biol. Chem.* **277**, 17781–17788
25. van den Akker, E., van Dijk, T. B., Parren-van Amelsvoort, M. P., Grossmann, K. S., Schaeper, U., Toney-Earley, K., Waltz, S. E., Lowenberg, B., and von Lindern, M. (2004) *Blood* **103**, 4457–4465
26. van Dijk, T. B., van den Akker, E., Amelsvoort, M. P., Mano, H., Lowenberg, B., and von Lindern, M. (2000) *Blood* **96**, 3406–3413
27. Kirsh, O., Seeler, J. S., Pichler, A., Gast, A., Muller, S., Miska, E., Mathieu, M., Harel-Bellan, A., Kouzarides, T., Melchior, F., and Dejean, A. (2002) *EMBO J.* **21**, 2682–2691
28. de Boer, E., Rodriguez, P., Bonte, E., Krijgsveld, J., Katsantoni, E., Heck, A., Grosveld, F., and Strouboulis, J. (2003) *Proc. Natl. Acad. Sci. U. S. A.* **100**, 7480–7485
29. Nishida, T., and Yasuda, H. (2002) *J. Biol. Chem.* **277**, 41311–41317
30. Starck, J., Mouchiroud, G., Gonnet, C., Mehlen, A., Aubert, D., Dorier, A., Godet, J., and Morle, F. (1999) *Exp. Hematol.* **27**, 630–641
31. Sachdev, S., Bruhn, L., Sieber, H., Pichler, A., Melchior, F., and Grosschedl, R. (2001) *Genes Dev.* **15**, 3088–3103
32. Tan, J. A., Hall, S. H., Hamil, K. G., Grossman, G., Petrusz, P., and French, F. S. (2002) *J. Biol. Chem.* **277**, 16993–17001
33. Hahn, S. L., Wasylyk, B., and Criqui-Filipe, P. (1997) *Oncogene* **15**, 1489–1495
34. Chung, C. D., Liao, J., Liu, B., Rao, X., Jay, P., Berta, P., and Shuai, K. (1997) *Science* **278**, 1803–1805
35. Liu, B., Liao, J., Rao, X., Kushner, S. A., Chung, C. D., Chang, D. D., and Shuai, K. (1998) *Proc. Natl. Acad. Sci. U. S. A.* **95**, 10626–10631
36. Arora, T., Liu, B., He, H., Kim, J., Murphy, T. L., Murphy, K. M., Modlin, R. L., and Shuai, K. (2003) *J. Biol. Chem.* **278**, 21327–21330
37. Liu, B., Gross, M., ten Hoeve, J., and Shuai, K. (2001) *Proc. Natl. Acad. Sci. U. S. A.* **98**, 3203–3207
38. Liu, B., Mink, S., Wong, K. A., Stein, N., Getman, C., Dempsey, P. W., Wu, H., and Shuai, K. (2004) *Nat. Immunol.* **5**, 891–898
39. Johnson, E. S., and Gupta, A. A. (2001) *Cell* **106**, 735–744
40. Roth, W., Sustmann, C., Kieslinger, M., Gilmozzi, A., Irmer, D., Kremmer, E., Turck, C., and Grosschedl, R. (2004) *J. Immunol.* **173**, 6189–6199
41. Wong, K. A., Kim, R., Christofk, H., Gao, J., Lawson, G., and Wu, H. (2004) *Mol. Cell. Biol.* **24**, 5577–5586
42. Santti, H., Mikkonen, L., Anand, A., Hirvonen-Santti, S., Toppari, J., Panhuysen, M., Vauti, F., Perera, M., Corte, G., Wurst, W., Janne, O. A., and Palvimo, J. J. (2005) *J. Mol. Endocrinol.* **34**, 645–654
43. Johnson, E. S. (2004) *Annu. Rev. Biochem.* **73**, 355–382
44. Girdwood, D., Bumpass, D., Vaughan, O. A., Thain, A., Anderson, L. A., Snowden, A. W., Garcia-Wilson, E., Perkins, N. D., and Hay, R. T. (2003) *Mol. Cell* **11**, 1043–1054
45. Ungureanu, D., Vanhatupa, S., Kotaja, N., Yang, J., Aittomaki, S., Janne, O. A., Palvimo, J. J., and Silvennoinen, O. (2003) *Blood* **102**, 3311–3313
46. Chun, T. H., Itoh, H., Subramanian, L., Iniguez-Lluhi, J. A., and Nakao, K. (2003) *Circ. Res.* **92**, 1201–1208
47. Gross, M., Yang, R., Top, I., Gasper, C., and Shuai, K. (2004) *Oncogene* **23**, 3059–3066
48. Lemarchandel, V., Ghysdael, J., Mignotte, V., Rahuel, C., and Romeo, P. H. (1993) *Mol. Cell. Biol.* **13**, 668–676